

A Further Discussion on Geometric
Errors of LANDSAT MSS Image

Wang Li

Institute of Seismology of State Seismological Bureau
People's Republic of China
Comission III

Abstract: This paper analyzes the geometric errors of five LANDSAT MSS images (two of them are successive) over the regions on different longitude and latitude of China by using the coordinate errors of the control points disposed along scan lines and in the along-track to plot the error curves of profiles in each direction. It has been found that the coordinate errors ΔY along X (which is identical with direction of scan lines) and the coordinate errors ΔX along Y (which is opposite to direction of track) in all the images present negative signs, systematically, and the error characteristics of the MSS image mainly depend on the influence of the platform attitude variations. Since there are different attitude variations in the different images, the different error curves are formed; however, the error curves in the successive images are similar, it shows that the attitude variations are slow. In this paper from the errors of images it is estimated that 700-800 m coordinate errors may be caused by the attitude variations.

1. The Characteristics of Geometric Errors in LANDSAT MSS Image

Obtained From the Samples

In order to analyze the geometric errors of MSS image, four images (two of them are successive on a same track) located in almost the same longitude and different latitude and two images located in almost the same latitude and different longitude are used. Their numbers and geographic coordinates are listed in Tab.1.

Tab.1

| Number | Serial No. of the LANDSAT Image | Geographic Coordinates | No. of Control Points |
|--------|---------------------------------|------------------------|-----------------------|
| A | E-1556-02115-5 | N50°18' E122°44' | 52 |
| B | E-1503-02225-5 | N37°22' E116°10' | 55 |
| C | E-1503-02232-5 | N35°57' E115°42' | 61 |
| D | E-1517-02030-5 | N25°57' E118°33' | 53 |
| E | E-1530-03171-5 | N25°59' E99°55' | 59 |

More than fifty control points have been identified in each image, and the numbers of identified control points in which the points with mistakes were discarded are given in Tab.1. All the points must be chosen along the same scan line and in the same along-track as well as possible and well-distributed over image. In fact, the images A, D and E are located in mountain areas, which have more outlines of image, therefore the points are distributed evenly. The other two images are located in flatlands, the distribution of the points is not enough well (refer to Fig.1)

Using the polyester fibre images, the coordinates of points in image are measured monocularly on the comparator. The origin of coordinate system is in the approximate image center, the y-axis points backwards along the nominal subsatellite track, the x-axis, which

is identical with direction of scan line, to the left of the track. The map coordinates of points are measured also on maps with scale of 1:100000 (most maps are arephotographed before 1960_s). Since the resolution of the MSS image is lower, in the process of measurement the location of point in image which are contacted by index mark are calibrated by comparing the maps so that the identification errors will be minimized.

The ground coordinates of points are computed as follows:

$$X_p = xM, \quad Y_p = yM \quad (1)$$

where X_p, Y_p are computed ground coordinates; x, y , measured image coordinates; M , the denominator of image scale estimated using the control points.

The following conformal transformation formulas are used to transform the map coordinates of points into the image coordinate system:

$$X_M = A_1X + A_2Y + A_3, \quad Y_M = -A_2X + A_1Y + A_4 \quad (2)$$

where X_M, Y_M are transformed coordinates; X, Y , measured coordinates on map; A_1, \dots, A_4 , transformation coefficients.

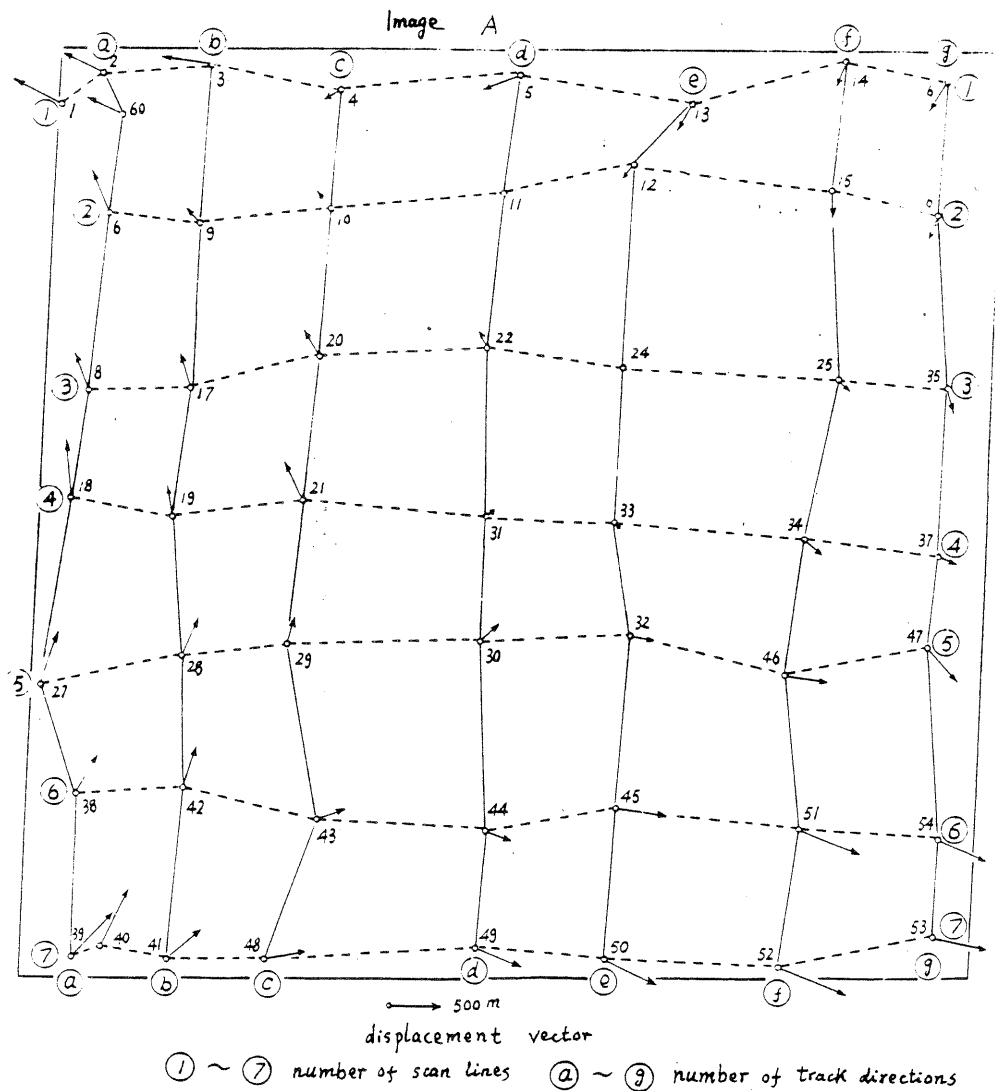


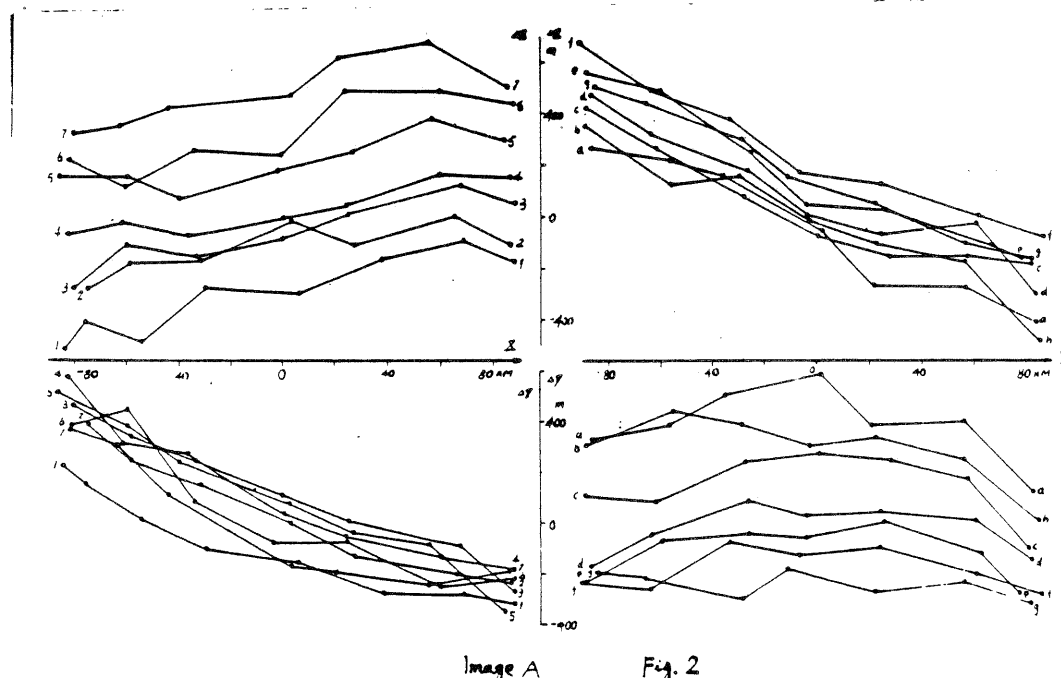
Fig. 1

The quality of the coordinate error distributions depends on the goodness or badness of transformation coefficients. In order to find the optimum coefficients, both map and computed coordinates of more than one-fourth points are used, and the solution is obtained by means of least squares method. Then the coordinate errors are:

$$\Delta X = X_p - X_M, \quad \Delta Y = Y_p - Y_M \quad (3)$$

The error vector distributions of image A are illustrated in Fig.1.

Since the conformal transformation only solves the problems of rotation and shift between the image and map coordinate systems, the obtained coordinate errors include all kinds of systematic and random errors. In order to understand the practical pattern of error distribution, the points in image are arranged in scan line and track direction approximately. The unified order of arrangement is shown in Fig.1. On the basis of the coordinate errors of points the ΔX and ΔY error curves of profiles in each direction are then plotted respectively (refer to Fig. 2-6). The amplitudes of curves in each direction are given in Tab. 2 (the amplitudes are maximum relative coordinate errors $\Delta X(am)$ and $\Delta Y(am)$ between both ends of each curve).



2. The Present Theoretic Analysis on Geometric Errors of LANDSAT MSS Image

There are many literatures discussing the geometric errors of LANDSAT image [4-8]. It is stated that following error sources are contained in MSS image in which the inner geometric errors of the linear skew and the non-linear mirror sweep are corrected [5]. a). The distortion along scan lines due to the panoramic sweep of the scanner and the earth curvature:

$$\Delta X_1 = [Ha^3(v^2+v)/6]t^3 \quad (4)$$

where H is the altitude of satellite above the earth surface (for LANDSAT, $H=920\text{km}$); $a=\max|\theta|/\max|t|$, θ is scan nadir angle, $\max|\theta|=0.1005$ rad., t is scan time, for one half of a scan line, $\max|t|=0.0165\text{s}$, thus $a=6.0942$; $v=(H+R)/R$, R is the earth radius (6368km).

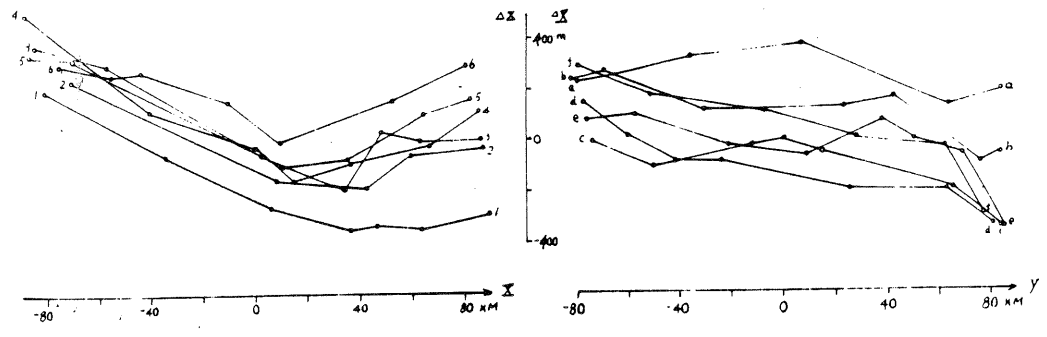


Image B
Fig. 3

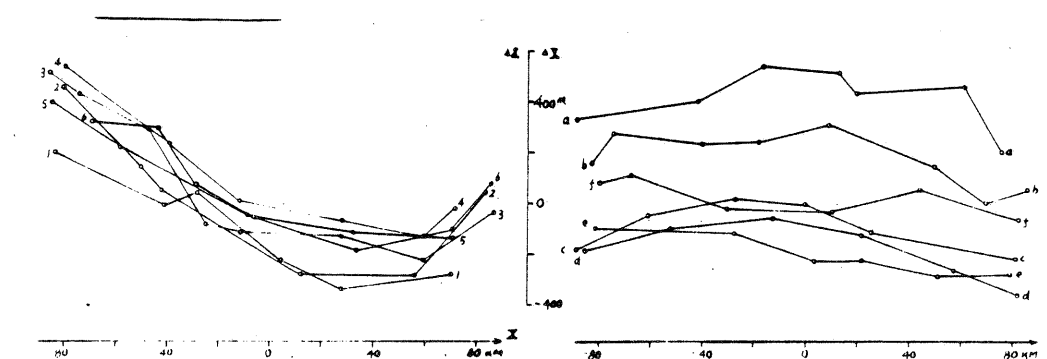
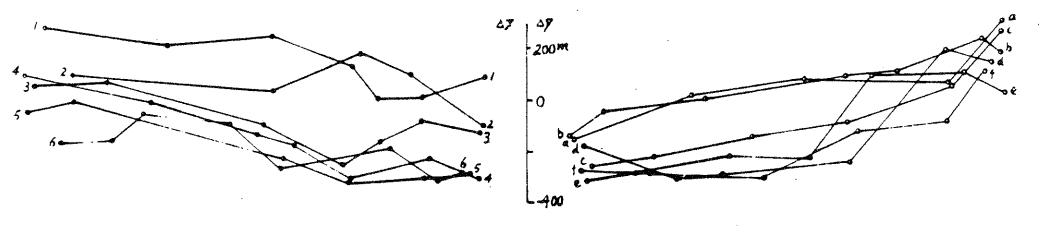


Image C
Fig. 4

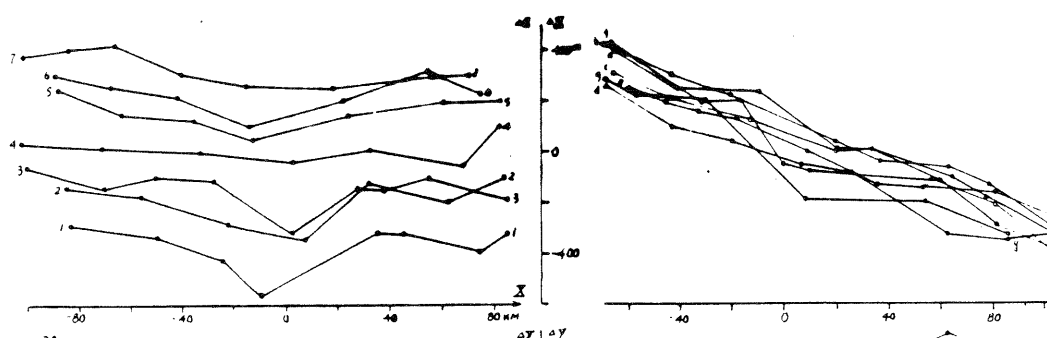
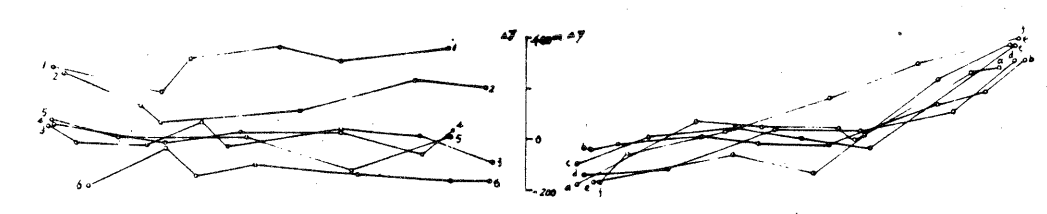
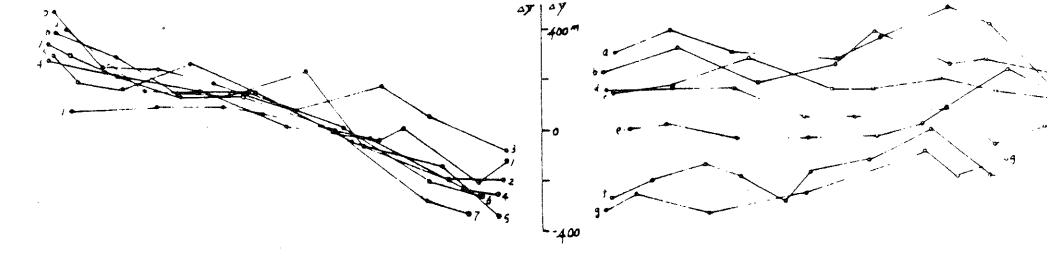


Image D
Fig. 5



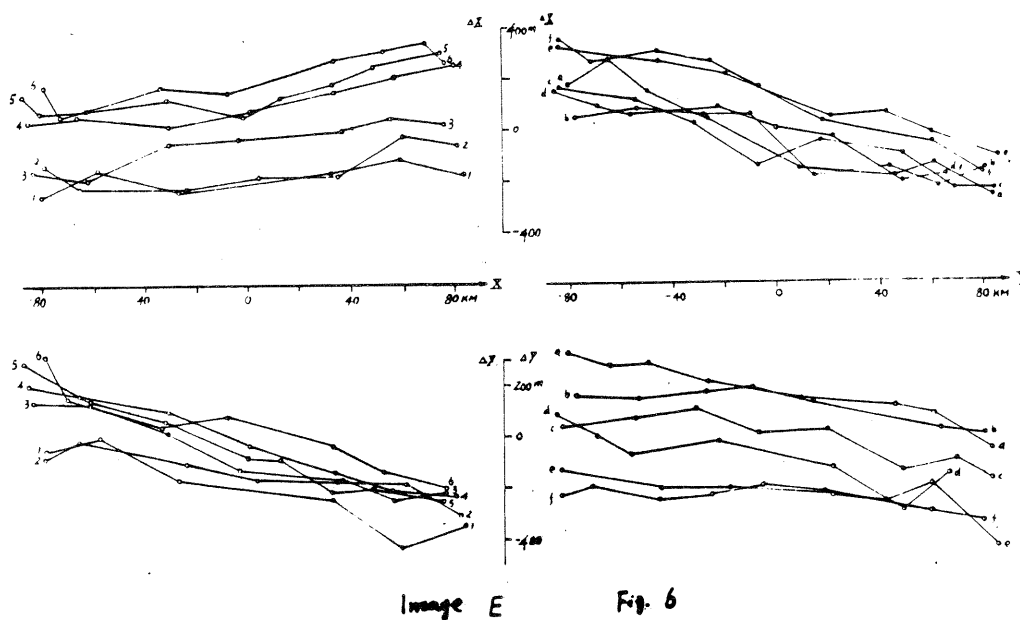


Image E

Fig. 6

Tab. 1

| No. of image | A | | | B | | | C | | | D | | | E | | | |
|-----------------|-------------------|-------------------|------------|-------------------|-------------------|------------|-------------------|-------------------|------------|-------------------|-------------------|------------|-------------------|-------------------|------------|-----|
| | $\Delta X_{(km)}$ | $\Delta Y_{(km)}$ | ΔS | $\Delta X_{(km)}$ | $\Delta Y_{(km)}$ | ΔS | $\Delta X_{(km)}$ | $\Delta Y_{(km)}$ | ΔS | $\Delta X_{(km)}$ | $\Delta Y_{(km)}$ | ΔS | $\Delta X_{(km)}$ | $\Delta Y_{(km)}$ | ΔS | |
| X buoys | 1 | +33 | -544 | 695 | -484 | -201 | 526 | -485 | 96 | 494 | -24 | -284 | 485 | 150 | -343 | 314 |
| | 2 | 279 | -637 | 695 | -261 | -208 | 334 | -402 | -57 | 406 | 32 | -605 | 606 | 180 | -382 | 422 |
| | 3 | 396 | -730 | 830 | -365 | -197 | 415 | -540 | -142 | 558 | -130 | -565 | 580 | 219 | -389 | 446 |
| | 4 | 232 | -764 | 798 | -383 | -408 | 560 | -548 | -10 | 598 | 61 | -527 | 531 | 228 | -435 | 491 |
| | 5 | 218 | -847 | 875 | -169 | -264 | 313 | -534 | -52 | 537 | -60 | -623 | 626 | 221 | -538 | 582 |
| | 6 | 287 | -657 | 717 | 2 | -123 | 123 | -235 | 23 | 236 | -73 | -657 | 661 | 395 | -550 | 677 |
| | 7 | 336 | -562 | 655 | | | | | | | -85 | -678 | 683 | | | |
| average | 312 | -677 | 752 | -277 | -235 | 378 | -457 | -24 | 463 | -40 | -563 | 567 | 232 | -440 | 499 | |
| Δ buoys | a | -671 | -200 | 700 | -42 | 452 | 454 | -129 | 555 | 570 | -694 | -138 | 706 | -538 | -365 | 650 |
| | b | -835 | -287 | 883 | -300 | 303 | 426 | -105 | 351 | 366 | -753 | -17 | 753 | -315 | -146 | 347 |
| | c | -598 | -214 | 635 | -346 | 515 | 620 | -40 | 458 | 460 | -742 | -37 | 743 | -415 | -204 | 462 |
| | d | -775 | 27 | 775 | -498 | 313 | 588 | -172 | 444 | 476 | -584 | -10 | 584 | -323 | -371 | 472 |
| | e | -730 | -103 | 747 | -425 | 329 | 537 | -185 | 528 | 559 | -572 | -41 | 573 | -428 | -303 | 524 |
| | f | -751 | 40 | 752 | -665 | 368 | 760 | -150 | 557 | 575 | -822 | 70 | 825 | -519 | -576 | 775 |
| | g | -669 | -128 | 687 | | | | | | | -610 | 201 | 672 | | | |
| | average | -718 | -135 | 738 | -379 | 380 | 560 | -130 | 482 | 501 | -682 | 4 | 689 | -423 | -327 | 542 |

$$* \Delta S = \sqrt{\Delta X^2 + \Delta Y^2}$$

b). The skewing and bending of lines in the along-track direction as well as the convergence of scan lines due to earth rotation and UTM map projection:

$$\Delta X_2 = -\frac{1}{2}(g/R)(L^2 - 2LY + Y^2) \quad (5)$$

$$\Delta Y_2 = (k/R)(-LX + XY) \quad (6)$$

where $g = dK/d\rho$ is the curvature of the real track; K is angle of the real track with respect to the due north; ρ , the travelling angle of satellite along the orbit relative to the vertex (the northernmost point of satellite); $k = dS/d\rho$ is the change of scan direction; and S , the scan line angle relative to map north in UTM plane; L , the ground distance corresponding to a half of picture side (for LANDSAT $L = \pm 92.5$ km).

c) The errors resulted from satellite platform attitude variations, which are more complex than others. The following Equations [2] of influence of attitude variations are developed by author from the propagation law of the outer orientation element errors in a long strip in photogrammetry [1] :

$$\Delta X_3 = \tan\theta dZ - H(1 + \tan^2\theta) d\phi + \frac{1}{2} Bdk + idX \tag{7}$$

$$\Delta Y_2 = -Hdw + H\tan\theta dk + \frac{1}{2} Hdw \tag{8}$$

where $d\phi$, dw and dk are the roll, pitch and yaw components of platform attitude variations respectively; dZ , dX , the displacements of LANDSAT; B , the distance between two successive scan lines (474m); i , the number of scan lines. Because $iB=Y$, $\tan\theta = \frac{X}{H}$, above Equations become:

$$\Delta X_3 = -Hd\phi + \frac{X}{H}dZ - \frac{X^2}{H}d\phi + \frac{Y}{B}dX + \frac{Y^2}{2B}dk \tag{9}$$

$$\Delta Y_2 = -Hdw + Xdk + Y^2 \frac{H}{2B^2} dw \tag{10}$$

The errors expressed by Eq.(4) are constant for each scan line. In Eq.(5) and (6), since the magnitude of g and k are related to the geographic latitude, the higher the latitude in north hemisphere, the greater the values of g and k will be, thus the resulting distortion increases with the increment of latitude. However for the images whose geographic location are known we can compute their theoretical errors. First the coordinate errors of twenty-five points which are distributed regularly in a hypothetic image are calculated from given Equations. The scan time 0, ± 8 and ± 16 ms are used for calculation of Eq.(4). The values of g and k of center meridian located in latitude of image A are used for calculation of Eq.(5) and (6) ($g=110 \times 10^{-3}$, $k=55 \times 10^{-3}$). For the sake of comparison, using the distortion coordinates, which maintain the coordinate errors, and theoretic coordinates the distortion coordinates are transformed conformally by Eq.(2); then the coordinate errors are computed from transformed distortional and theoretic coordinates; by using the coordinate errors of each point along scan line and track, the theoretical error curves of profiles are finally plotted (refer to Fig.7). The amplitude values of each error curves presented in Tab.3.

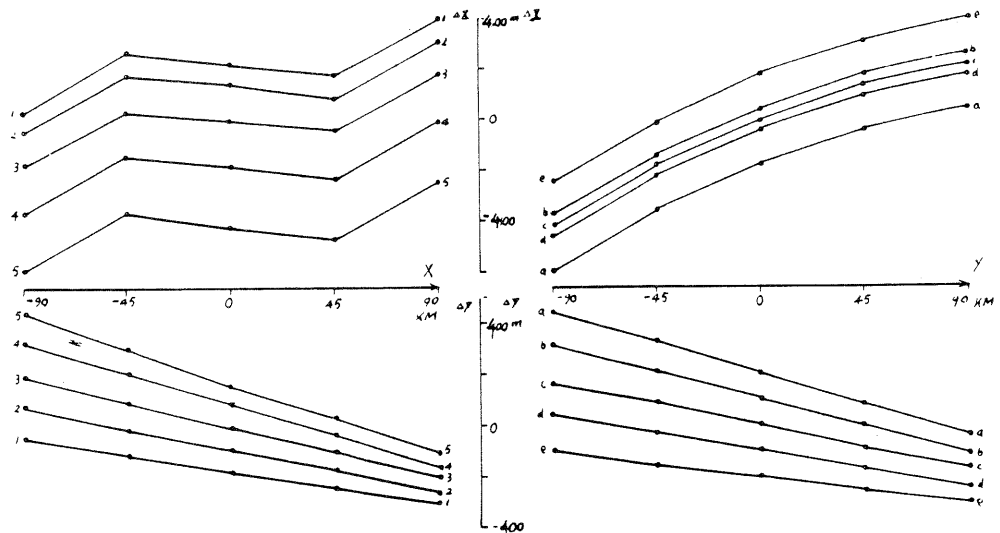


Fig. 7

Tab.3

| | | $\Delta X(\text{am})$ | $\Delta Y(\text{am})$ | ΔS | | | $\Delta X(\text{am})$ | $\Delta Y(\text{am})$ | ΔS |
|------------|---|-----------------------|-----------------------|------------|------------|---|-----------------------|-----------------------|------------|
| along X | 1 | 350 | -262 | 473 | along Y | a | 638 | -496 | 808 |
| | 2 | 350 | -336 | 485 | | b | 638 | -422 | 765 |
| | 3 | 350 | -410 | 539 | | c | 638 | -348 | 727 |
| | 4 | 350 | -484 | 597 | | d | 638 | -274 | 694 |
| | 5 | 350 | -538 | 659 | | e | 638 | -200 | 669 |
| average | | 350 | -410 | 543 | average | | 638 | -348 | 733 |

By comparing Fig.7 with Fig.2-6 and Tab.2 with Tab.3, the following things can be seen:

(1).The coordinate errors ΔX along X (which is identical with scan lines) in images A and E present systematically positive, which are a little similar to the theoretical values, it indicates that the errors caused by the panoramic sweep and earth curvature may be included in image, but it isn't affirmable from other images which have not the same systematic errors. *)

(2).The coordinate errors ΔY along X of all the images present negative signs systematically, and the ΔY error curves along Y (which is opposite to direction of track) of most images (such as A, D and E) shift down in the sequence of numbers in Fig.1. which are similar to the theoretical curves; therefore it is possible that the image contains the errors due to the earth rotation and UTM map projection. However, the coordinate errors ΔX along Y of all the images present negative signs systematically and the ΔX coordinate curves along X of most images shift up in the sequence of numbers in Fig.1, which are different from theoretical curves, it shows that some other sources which cause such systematic errors may be included in image.

(3).The systematic errors of different images are not the same, as if it is independent of geographic latitude of image, and the patterns of error curves of different images are not the same too, specially for the curves of images B and C, which are rather different from Fig.7, these ought to result from the influence of platform attitude variations.

(4).The pattern and its change of error curves in successive images are coincidence with each other, it may be that the process of attitude variation is slow.

3.The Description of the Geometric Errors of LANDSAT MSS Image
By means of plotting the error curves of profiles and comparing the real error curves in five images with theoretical one, we not only have understood the characteristics of error curves of image, but also found the size of relative point errors (which is 500-700m in general and the maximum value can be 900m from the ΔS of Tab.2) in an image. Besides the systematic errors, there are even more the random errors in the geometric errors of image. The latter are mainly caused by attitude variations. Moreover the

*) Through comparison it is found that the image doesn't perhaps contains the errors caused by the panoramic sweep etc., but now we still compare the error curves of real images with Fig.7, however the coordinate errors ΔX along X in Fig.7 are assumed to be the results from modeling the influence of a certain attitude variation component.

error property of image mainly depends on the random errors which cause not only distortion of the inherent systematic error in an image, but also the considerable non-linear errors.

The Eq.(9) and (10) also show that the attitude variations can cause the errors in Y coordinate as well as in X coordinate. For instance, in Eq.(9), $d\phi$ and dZ can cause errors in X coordinate along X which will form various error curves of profiles and dk and dX can cause up or down shifting to each profile curve in respective direction.

Since the attitude variations are random, different image has different attitude variation, which will lead to different error curves. However the process of attitude variation may be slow as viewed from the similarity of error curves in successive images. Although the exact values of attitude variations have not yet been obtained, the magnitude of the errors which may be resulted from attitude variations and the attitude variations which may be occurred in an image, can be estimated approximately from the relative difference of amplitude between two images. Assuming the average amplitudes in Tab.2 to be the errors compounded basically by both systematic and random errors as stated above in respective image, the difference of amplitude between two images can be considered as errors due to the attitude variations. For example, from Tab.2, one find the maximum difference of amplitude of coordinate error ΔX along X: $\Delta X(s) = \Delta X(am)_c - \Delta X(am)_A = -457 - 312 = -769m$, and the maximum difference of amplitude of coordinate error ΔY along Y: $\Delta Y(t) = \Delta Y(am)_E - \Delta Y(am)_C = -327 - 482 = -809m$ (this difference contains the error caused the earth rotation and UTM map projection due to the difference of latitude, but since the difference of latitude between image C and E is very small, only 10° , it can be considered as the error resulted from the attitude variations). Hence it may be concluded that the platform attitude variations can cause 700-800m coordinate errors to MSS image.

For the successive images, from Tab.2, it can be found that the differences of amplitude of coordinate errors ΔX and ΔY along X are: $\Delta X(s) = -457 - (-277) = -180m$, $\Delta Y(s) = -24 - (-235) = 211m$; and the differences of amplitude of coordinate errors ΔX and ΔY along Y are: $\Delta X(t) = -130 - (-379) = 249m$ and $\Delta Y(t) = 482 - 380 = 102m$. In view of the fact that the relativity of influences of $d\phi$ and dZ , dk and dX to the coordinate errors, which can be found from Eq.(9), but in Eq.(10) only the influence of dw to ΔY error profile curves along Y can be found, and the dk only effects the shift of profile curves, thus by using the difference of amplitude between successive images the attitude variations which may be existed in an image can be estimated by right hand third and fourth terms of Eq.(10):

$$dk = \frac{\frac{1}{2} \Delta Y(s)}{X} \rho \approx 4', \quad dw' = \frac{\Delta Y(t)}{i^2 H} \times 2 \times \rho \approx 0.3ms.$$

The obtained dw' is the pitch variation which may be existed in each band-picture at sweeping instant. As a result, on the average meaning, for a MSS image, the pitch variation can be $dw \approx 23''$. Hence the variation process of platform attitude is gradual and slow.

Because of the slow speciality of the attitude variations, there exists approximate similarity among the error curves of profiles along X and Y of an image. However, because of the elevation difference on ground, measurement and identification errors, the ground change between the aerophototopography and the NSS imagery in tens years (especially for flatland) and the deviation of points from the assigned direction, etc., a few points of the curves are led to jump (within about $\pm 100\text{m}$).

Finally, it should be noted that, as stated above, the coordinate errors ΔY along X and coordinate errors ΔX along Y of all the images present negative signs systematically, which result in image distortion shown in Fig.8. In addition, from the differences between the diagonal scale of images (refer to Tab.4,), it is found that the diagonal scale of left-up to right-down in images is less than that of the left-down to right-up, except image C. It shows that there certainly exists skew in images. For the purpose of comparing, the scales of both diagonals of theoretical error image are listed in Tab.4, their difference are just opposite to real ones.

Tab. 4

| No. of image | Denominator of Scale | |
|---------------------|----------------------|--------------------|
| | left-up~right-down | left-down~right-up |
| A | 998410 | 990458 |
| B | 996860 | 993880 |
| C | 996208 | 996937 |
| D | 999177 | 993887 |
| E | 999122 | 991962 |
| theore. error image | 1001300 | 1002570 |

* The scales of each direction of each image are the means estimated from more than two pairs of points.

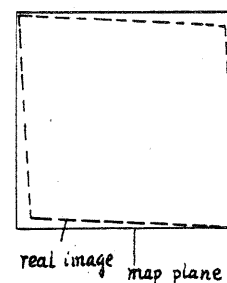


Fig. 8

In above systematic errors, the systematic negative signs of coordinate errors ΔY along X are to be the influences of the earth rotation and UTM map projection, but the resource causing the systematic negative signs of coordinate errors ΔX along Y is not yet understood. As the fact is that the skew direction of real images is opposite to the direction of skew resulted from the earth rotation ($\Delta x = -D r_{\omega} \cos \theta \sin \rho_0$, By reference to the Eq.15 in [7]), it seems to be considered that the image skew is over-corrected in rough treatment, (For instance, the designed LANDSAT orbit is a near-polar circular one, but in fact it can not be a exact circular, the angular velocity of LANDSAT in its orbit is probably changeable) or there are other unknown reasons. In addition, are there the same systematic errors in images over other regions on earth (for example, the equator or the southern latitude)? For answers these questions, further experiments and study with global cooperation are necessary.

4. Conclusion

On the basis of analysis of the LANDSAT MSS image in China, the preliminary conclusion is obtained as follows:

(1). Besides the systematic errors resulted from earth rotation etc., a more important source of the geometric error in the LANDSAT MSS rough image is the influence of platform attitude variations, which can cause 700-800m non-linear random coordinate errors, and determine the characteristics of error curves. Since there are different attitude variations in different images, the different error curves in different images are formed. But the error curves of the successive images on a same track are similar, it shows that the process of the attitude variation is slow.

(2). The systematic errors of LANDSAT MSS image in China are: the coordinate errors ΔY along X and coordinate errors ΔX along Y present negative signs systematically. Whether there exists the same in other regions on earth? It is necessary to experimentize with global cooperation.

(3). The error curves of each direction can be obtained by analyzing geometric errors of image from plotted error curves of profiles. It provides the reliable basis for the fine treatment of MSS image by using polynomial to model the errors of an image [3,4].

References

1. Wang Zhizhuo, Principle of Photogrammetry. Surveying and Mapping Press. Beijing, pp.55-59. 1980.
2. Wang Li, Yang Xiafang and Jiang Chunming, A Discussion on Geometric Errors of ERTS MSS Image. Journal of Surveying and Mapping, Vol.13 No.3, pp.199-207, 1983.
3. Wang Li, A Discussion of Rationality of Polynomial Correction Formulae of LANDSAT MSS Image. Crustal Deformation and Earthquake. 1981.
4. Konecny, G., Remote Sensing Technique. A Lecture Note Presented at College of Geodesy, Photogrammetry and Cartography, 1980.
5. Steiner, D. and Kirby, M.E., Geometric Referencing of LANDSAT by Affine Transformation and Overlaying of Map Data. Photogrammetria. No.2 1977.
6. Derenyi, E.E. and Konecny, G., Infrared Scan Geometry. Photogrammetric Engineering. No.5 1966.
7. Kratky, V., Cartographic Accuracy of ERTS. Photogrammetric Engineering. No.2, 1974.
8. Horn, B.K.P. and Woodhan, R.J., LANDSAT MSS Coordinate Transformations. 5th Annual Symposium on Machine processing of Remotely Sensed Data. June 27-29, 1979.